

Recurrence in a periodically driven and weakly damped Fermi-Pasta-Ulam-Tsingou chain

Yujun Shi* and Haijiang Ren

*College of Physics and Electronic Engineering,
Shanxi University, Taiyuan 030006, China*

arXiv:2510.06568v1 [cond-mat.stat-mech] 8 Oct 2025

Abstract

We report numerical evidence of Fermi-Pasta-Ulam-Tsingou (FPUT)–like recurrence in weakly damped, periodically driven α -FPUT chains. In narrow regions of driving amplitude and damping, energy is quasi-periodically exchanged among a few low-frequency modes over long timescales. Unlike discrete time crystals, the recurrence period is not an integer multiple of the driving period and does not correspond to spontaneous symmetry breaking, yet it may suggest a generalized, relaxed form of time-crystalline-like order. The maximum damping allowing recurrence decreases rapidly with chain length, suggesting that in the thermodynamic limit such behavior is unlikely to persist. These results reveal a new type of coherent nonlinear dynamics in driven, open multimode systems and provide guidance for experimentally realizing long-lived quasi-periodic states.

I. INTRODUCTION

Fermi–Pasta–Ulam–Tsingou (FPUT) recurrence is a nonlinear phenomenon in multimode systems, where energy is exchanged primarily among a few low-frequency modes and quasi-periodically returns close to its initial distribution, instead of rapidly equi-partitioning across all modes[1–4]. As one of the celebrated problems in nonlinear science, it has attracted extensive theoretical and numerical investigation since its original report by Fermi, Pasta, Ulam, and Tsingou in 1953[1]. The prevailing understanding today is that the system eventually thermalizes and reaches energy equipartition, albeit over exceedingly long timescales[5, 6]. Thus, the recurrence is now viewed as a long-lived metastable regime, can be referred to as a prethermalized state[7].

Experimentally, observing FPUT recurrence remains highly challenging. To date, only a few reports have demonstrated recurrence-like behavior in various nonlinear systems, such as LC circuits, surface gravity waves, magnetic film-based active feedback rings, optical microresonators, and optical fibers[8–14]. However, in all these cases, the observed recurrence typically lasts for only a single cycle and occurs no more than three times[14]. One of the main obstacles is dissipation. FPUT recurrence was originally predicted for idealized Hamiltonian systems with strict energy conservation. In contrast, real physical systems inevitably involve dissipation, which severely limits the possibility of observing multiple recurrence

* yujunshi@sxu.edu.cn

cycles[15], as illustrated in Fig.1. Consequently, if one adopts the criterion of sustained recurrence over many cycles, it is reasonable to conclude that a genuine long-time FPUT recurrence has yet to be achieved experimentally.

Given that dissipation is unavoidable in most real physical systems, a natural question arises: can external driving compensate for energy loss and enable recurrence-like behavior? Specifically, can a dissipative, multimode nonlinear system—when subject to periodic forcing, exhibit a periodic or near-periodic response over timescales far exceeding the driving period, with energy predominantly exchanged among a small subset of modes, in a manner reminiscent of the original FPUT recurrence?

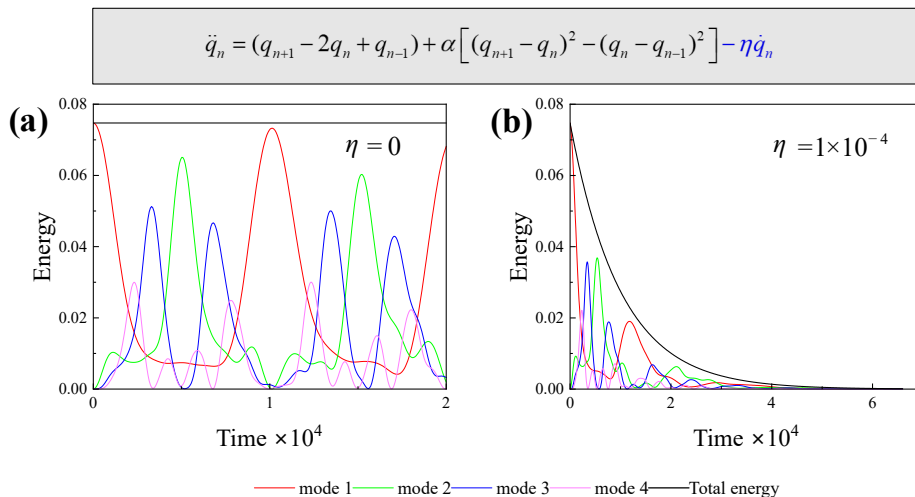


FIG. 1. (a) The FPUT recurrence in a chain of length $N = 32$ with $\alpha = 0.25$. (b) Multiple recurrence cycles are suppressed even when a small damping $\eta = 1 \times 10^{-4}$ is introduced.

It is well known that multimode nonlinear systems, involving many degrees of freedom, exhibit a rich variety of dynamical behaviors. As a representative example, consider a one-dimensional chain of anharmonic oscillators under periodic driving. When the driving frequency lies within the spectral band of the system's linear dispersion relation and the driving amplitude is small, the system behaves similarly to its linear counterpart: primary resonance peaks emerge near the eigenfrequencies of the normal modes, and the response is a steady-state oscillation synchronized with the driving period. As the driving amplitude increases, nonlinear effects become more pronounced, leading to the appearance of secondary resonances in the vicinity of the primary ones. In this regime, the system may exhibit not only periodic responses but also quasi-periodic or even chaotic dynamics[16]. When the

driving frequency lies outside the linear spectrum, for instance, near the band edge, the system can display more intricate dynamical phenomena, such as anharmonic waves, solitons, and breathers[17–22]. However, to the best of our knowledge, no FPUT-like recurrence involving multiple modes has been reported in such driven and damped chains. Nonstationary responses, characterized by periodic or quasiperiodic energy exchange, have so far been observed only in two-mode nonlinear systems[23–25].

As shown in this work, a key reason for the absence of such observations lies in the magnitude of the damping. In most previous studies of driven, damped anharmonic chains, the damping coefficient was typically chosen to be relatively large—often not smaller than 0.1—to accelerate convergence to a steady state in numerical simulations[16, 19–21]. Our results demonstrate that the emergence of robust recurrence behavior requires much smaller damping.

In this Letter, we present numerical evidence that a recurrence-like phenomenon can emerge in a periodically driven, weakly damped Fermi-Pasta-Ulam-Tsingou (FPUT) chain. Specifically, near the first mode, we identify a narrow region in the parameter space of driving amplitude and damping where energy is periodically exchanged among a few modes over long timescales. The maximum damping that allows such recurrence decreases rapidly with system size—for example, it is approximately 4.3×10^{-3} for $N = 8$, and about 5×10^{-5} for $N = 32$. These results suggest that in the thermodynamic limit, such recurrence behavior is unlikely to persist. We interpret this phenomenon as a new type of coherent nonlinear dynamics enabled by a delicate balance between weak driving, weak damping, and the system’s modal structure.

The paper is organized as follows. Section II introduces the model and the methodology used in our numerical simulations. Section III presents the numerical results, including representative recurrence phenomena and the dependence of the system’s response on driving frequency, driving amplitude, damping, and chain length. Finally, Sec. IV discusses the connection between the observed recurrence behavior and the recently explored concept of time crystals.

II. MODEL AND METHODOLOGY FOR OUR NUMERICAL SIMULATIONS

The equations of motion of the forced and damped α -FPUT chain are

$$\begin{aligned} \ddot{q}_n = & (q_{n+1} - 2q_n + q_{n-1}) + \alpha [(q_{n+1} - q_n)^2 - (q_n - q_{n-1})^2] \\ & - \eta \dot{q}_n + F \cos(\Omega t), \quad (n = 1, 2, \dots, N), \end{aligned} \quad (1)$$

where η is the damping coefficient, F and Ω are the amplitude and frequency of the driving force. The fixed boundary conditions are chosen: $q_0 = q_{N+1} = 0$.

We integrate Eq. (1) using a Runge-Kutta algorithm (verified with both MATLAB's `ode45` and Python's `scipy.integrate.solve_ivp`, yielding consistent results), with initial conditions $q_n = 0$ and $\dot{q}_n = 0$. In the original FPUT problem, Runge-Kutta methods are generally not used because they are not symplectic and therefore do not guarantee long-term energy conservation. In our driven-damped model, however, symplectic algorithm is not required. To minimize the influence of numerical errors, we set the solver's error tolerances smaller than the default values (e.g., relative error tolerance = 10^{-8} , absolute error tolerance = 10^{-12}).

we have monitored the hamiltonian of the undriven, undamped α -FPUT as the "total energy"

$$H = \sum_{n=1}^N \frac{p_n^2}{2} + \sum_{n=0}^N \left[\frac{1}{2} (q_{n+1} - q_n)^2 + \frac{\alpha}{3} (q_{n+1} - q_n)^3 \right], \quad (2)$$

and energies of the individual normal modes

$$E_k = \frac{P_k^2 + \omega_k^2 Q_k^2}{2}, \quad (3)$$

where the normal-mode frequencies are given by

$$\omega_k = 2 \sin \left(\frac{k\pi}{2(N+1)} \right), \quad (4)$$

and the normal-mode coordinates (Q_k, P_k) are related to the lattice coordinates (q_n, p_n) via

$$\begin{bmatrix} q_n \\ p_n \end{bmatrix} = \sqrt{\frac{2}{N+1}} \sum_{k=1}^N \begin{bmatrix} Q_k \\ P_k \end{bmatrix} \sin \left(\frac{nk\pi}{N+1} \right). \quad (5)$$

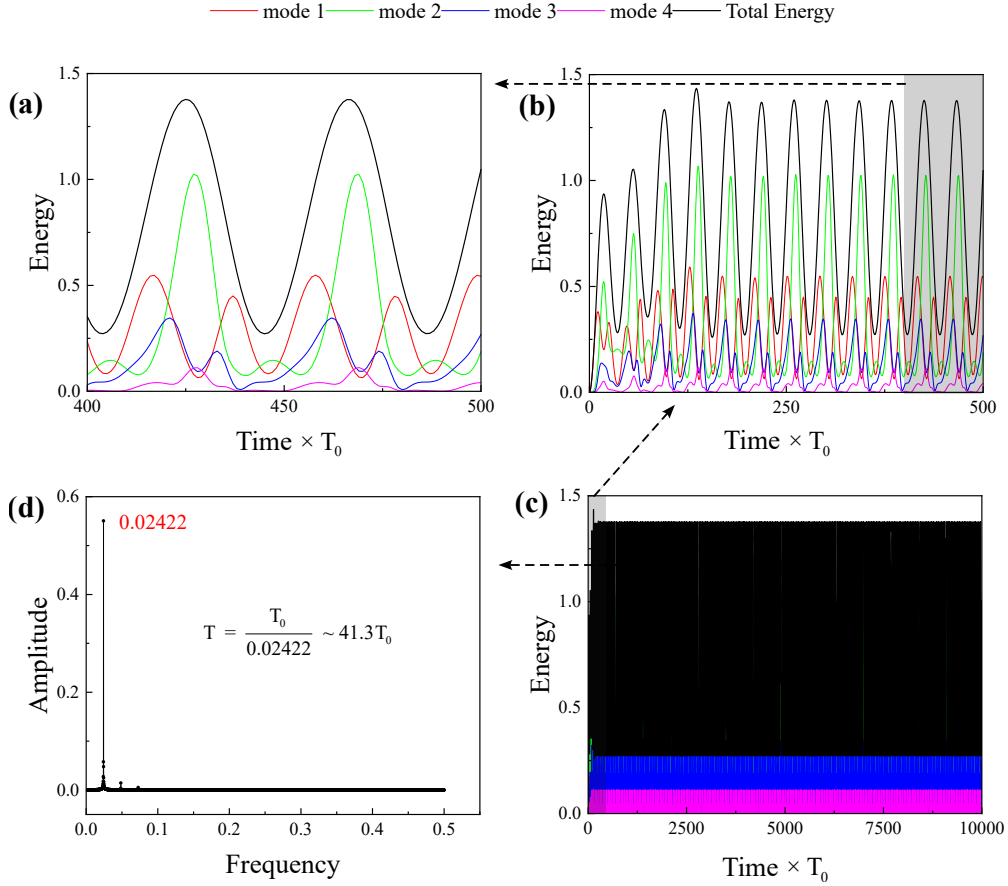


FIG. 2. Representative recurrence phenomenon. (a–c) Simulation results for the $N = 8$ chain with $\eta = 2.5 \times 10^{-3}$, driving amplitude $F = 5 \times 10^{-3}$, and driving frequency $\omega = 0.347$ (close to the first mode $\omega_1 = 0.3473$). The horizontal axis represents time in units of the driving period T_0 . (d) Fast Fourier transform (FFT) of the steady-state response shown in panel (c).

III. NUMERICAL RESULTS

Unless otherwise stated, all simulation results presented in this paper correspond to a chain of length $N = 8$ with a nonlinear coupling coefficient $\alpha = 0.25$.

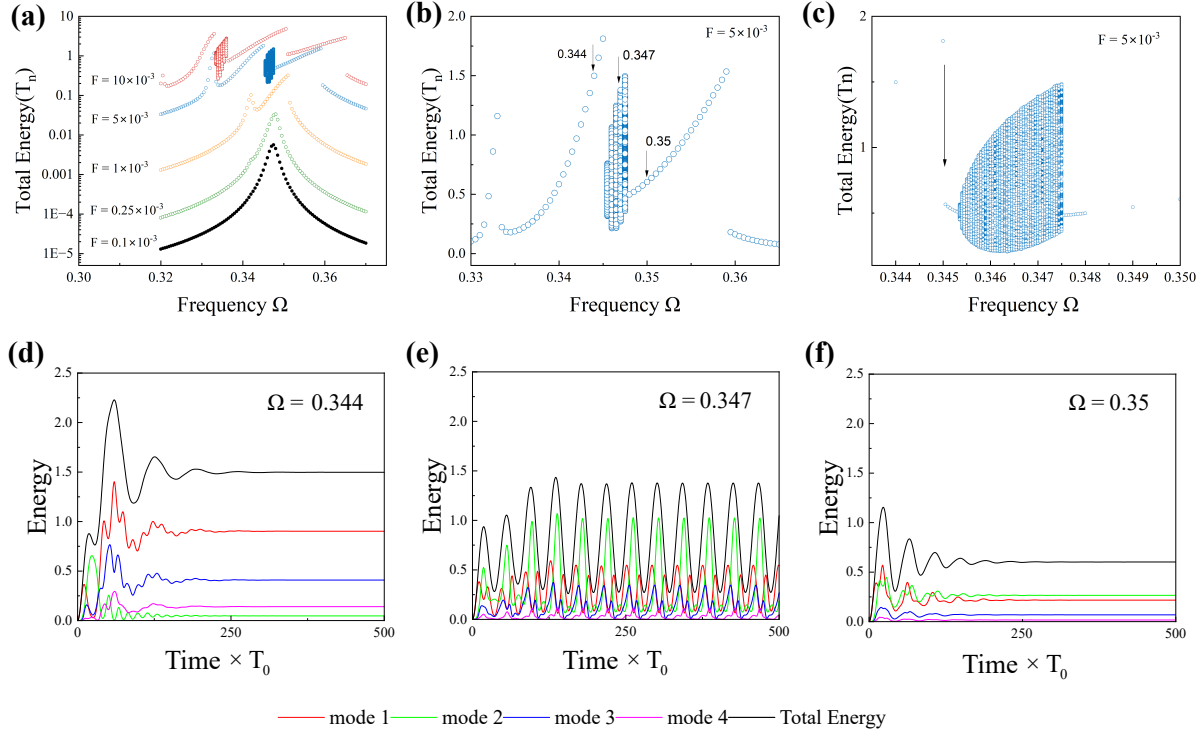


FIG. 3. (a) Total energy spectra of the $N = 8$ chain as a function of the driving frequency near the first mode $\omega_1 = 0.3473$, for different driving amplitudes. (b) The same data for $F = 5 \times 10^{-3}$ shown separately, with a linear scale on the vertical axis. (c) Enlarged view of the frequency range where the recurrence phenomena occur, obtained from a finer frequency scan of the section shown in (b). (d-f) Time-domain simulations for three representative driving frequencies.

A. Recurrence behavior at $\eta = 2.5 \times 10^{-3}$

1. Representative recurrence behavior

Figure 2 shows a representative recurrence behavior for a driving amplitude $F = 5 \times 10^{-3}$ and a driving frequency $\omega = 0.347$ (near the first mode $\omega_1 = 0.3473$). Instead of reaching a steady response, there is a continual exchange of energy between the low-frequency modes, exhibiting an almost periodic behavior with a period of approximately $41.3 T_0$ (T_0 is the driving period).

2. Energy spectra versus driving frequency

Figure 3(a) shows the total energy response as a function of the driving frequency near the first mode, $\omega_1 = 0.3473$, for different driving amplitudes. Specifically, for each set of control parameters, Eq. 1 was integrated for N driving periods T_0 (typically $N = 2000$) until transients had decayed. The total energy was then stroboscopically sampled with period T_0 over the following $500 T_0$, and these data points are plotted in Fig. 3(a). To maintain consistency, the first sampled point for each frequency scan was taken at the maximum total energy within one T_0 period.

As the driving amplitude increases, nonlinear effects become more pronounced, giving rise to secondary resonances near the primary peaks, accompanied by jump phenomena in their vicinity. The recurrence phenomena occur in the vicinity of these jumps, which is more clearly seen in Fig. 3(b) and (c). On both sides of the recurrence regions, the system still exhibits normal steady-state oscillations synchronized with the driving period (Figs. 3(d) and (f)).

A closer look at the recurrence phenomenon at $\Omega = 0.347$, particularly in Fig. 2(a), reveals that the average energy of mode 2 exceeds that of mode 1. Given that $\omega_2 = 0.684 \sim 2\omega_1$, one may speculate that this recurrence arises because the driving at $\omega = 0.347$ simultaneously excites mode 1 (primary resonance) and mode 2 (secondary, specifically a super-harmonic resonance). The phase mismatch and mutual coupling between these modes lead to periodic energy exchange among them. We can exclude this possibility that the driving simultaneously injects energy into both mode 1 and mode 2. This is because our uniform driving field is even symmetry with respect to the chain center; consequently, whether it is the primary or secondary resonance, only modes with the same spatial symmetry can be directly excited. Direct energy injection into odd-symmetric even-numbered modes is forbidden. This is illustrated in Fig. 4(a), which shows the total energy spectra over a wider driving frequency range (from 0.32 to 2) with $F = 5 \times 10^{-3}$. Only the primary resonances corresponding to odd-numbered modes are excited. Therefore, the only pathway for energy injection is through the initial excitation of mode 1, followed by transfer to higher-order modes via nonlinear coupling, ultimately resulting in a recurrence characterized by a dynamic balance among the low-frequency modes.

Figure 5 shows the energy response for $F = 10 \times 10^{-3}$, which corresponds to one of

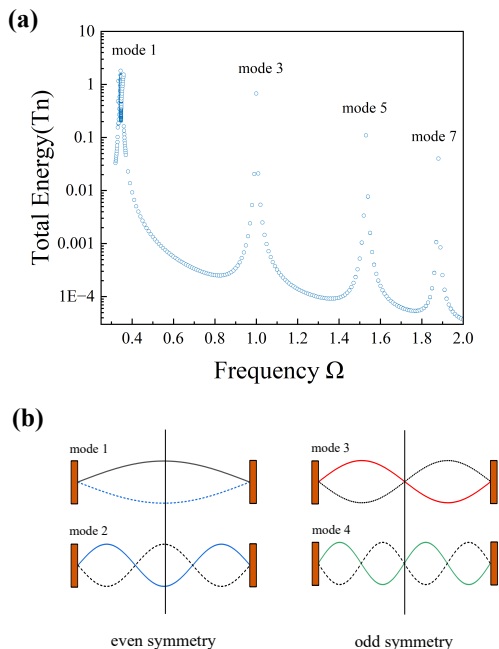


FIG. 4. (a) Total energy spectra of the $N = 8$ chain as a function of the driving frequency from 0.32 to 2, for the driving amplitudes $F = 5 \times 10^{-3}$. Because the chain is driven uniformly, only modes with even spatial symmetry about the chain center are excited, so the primary resonance peaks appear only near the odd-numbered mode frequencies. (b) Spatial symmetry of the normal modes.

the data traces in Fig. 3(a) plotted separately for clarity. The recurrence phenomenon at $\Omega = 0.335$ [see Fig. 3(b)] indicates that the energy is mainly concentrated in modes 1 and 3, in contrast to the case of $F = 5 \times 10^{-3}$, where modes 1 and 2 dominate.

In addition to the uniform driving, we also examined two other types of excitation: a single-site driving $F_n = a \delta_{n,n_0} \sin(\Omega t)$ and a mode-matched driving $F_n = a \sin\left(\frac{nk\pi}{N+1}\right) \sin(\Omega t)$. Both cases produce similar recurrence behaviors, indicating that the recurrence is an intrinsic consequence of the system's nonlinear mode coupling rather than a specific feature of the uniform excitation.

3. Energy spectra versus driving amplitude

To further examine how the driving amplitude influences the excitation dynamics, an amplitude scan was performed at $\Omega = 0.347$ [Fig. 6]. At low amplitudes ($F = 1 \times 10^{-3}$),

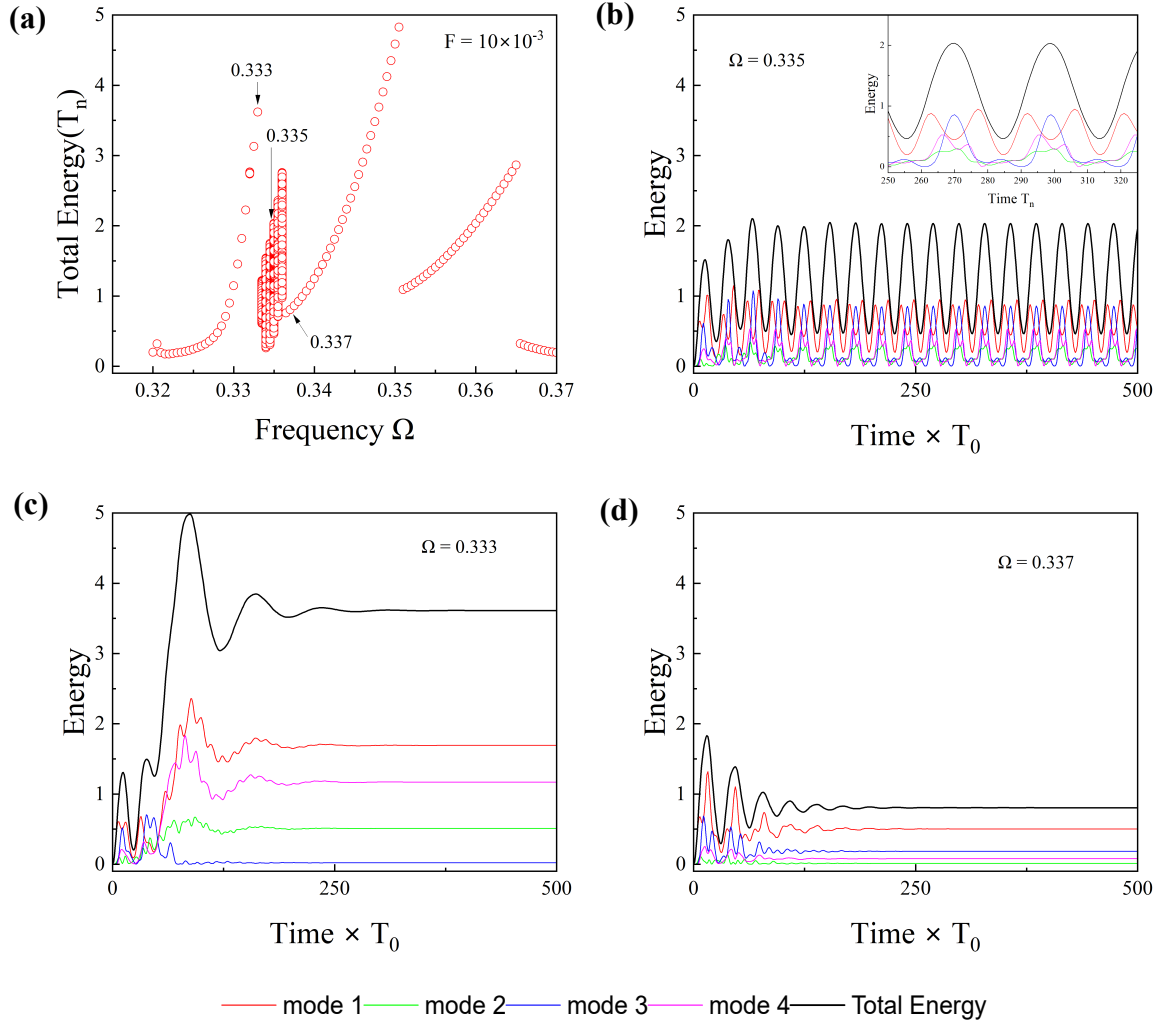


FIG. 5. (a) Total energy spectra of the $N = 8$ chain as a function of the driving frequency near the first mode $\omega_1 = 0.3473$, for driving amplitudes $F = 10 \times 10^{-3}$. (b-d) Time-domain simulations for three representative driving frequencies.

the system exhibits normal steady-state oscillations dominated by mode 1. With increasing amplitude, enhanced nonlinear coupling between modes 1 and 2 causes the energy to shift gradually toward mode 2, which becomes dominant in the recurrence region. Beyond this region, the system resumes normal steady-state oscillations, again dominated by mode 1.

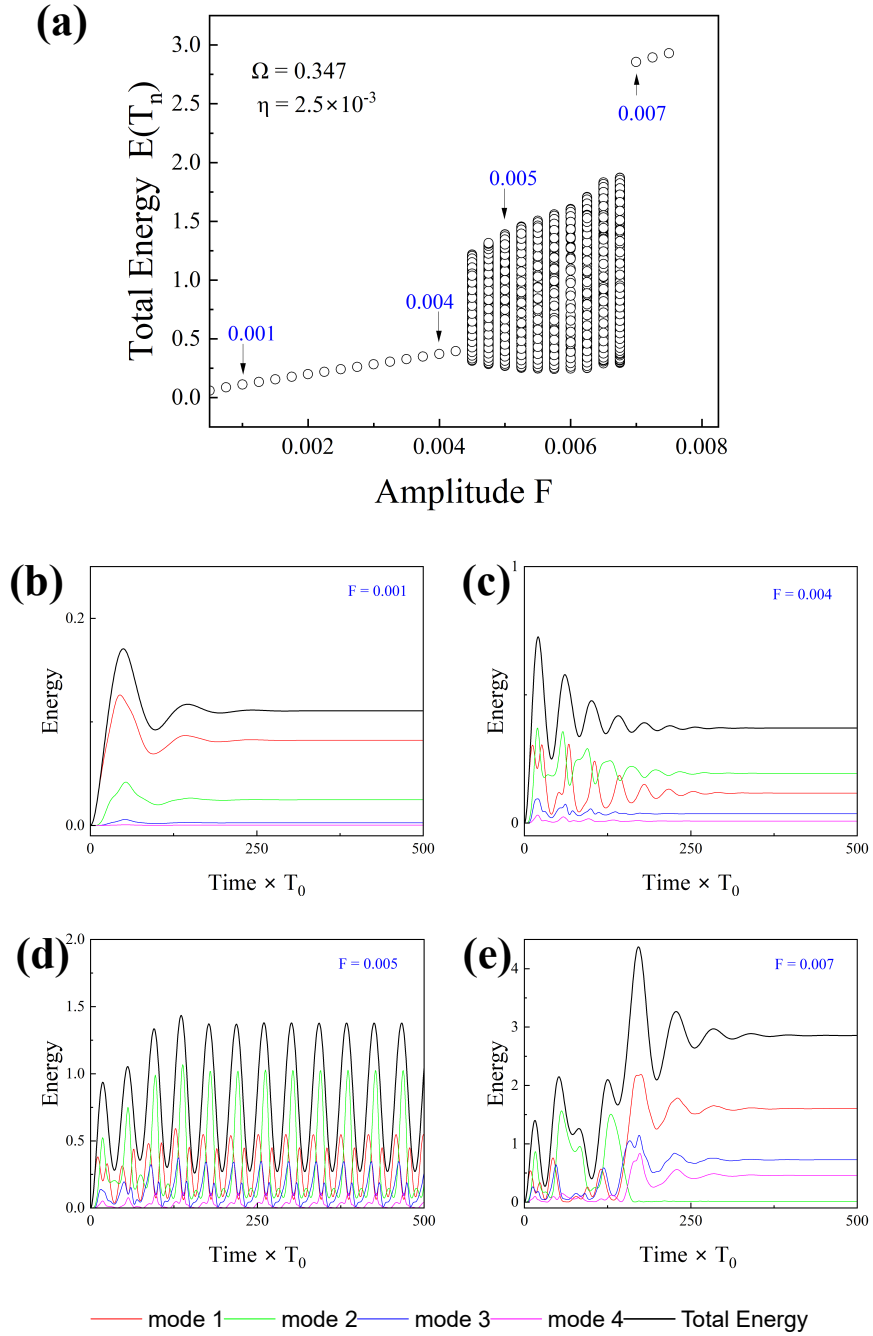


FIG. 6. (a) Total energy spectra of the $N = 8$ chain as a function of the driving amplitude at the driving frequency $\Omega = 0.347$. (b-e) Time-domain simulations for four representative driving frequencies.

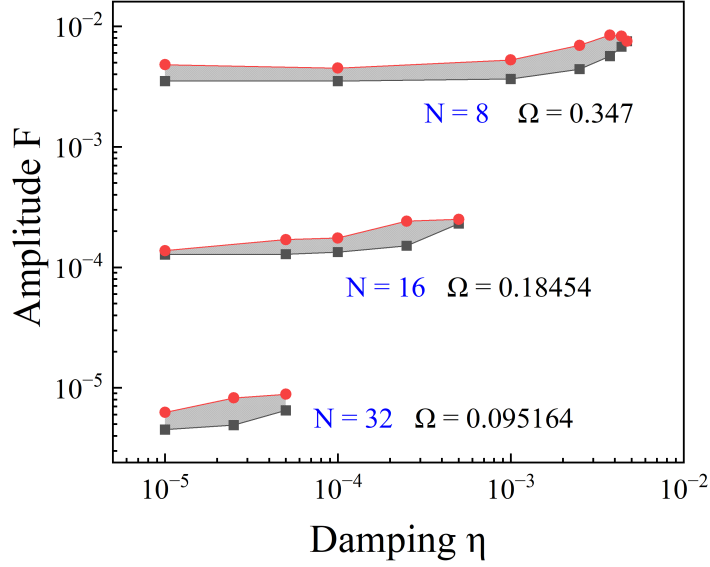


FIG. 7. Recurrence regions in the driving amplitude–damping plane for chains of length $N = 8$, 16, and 32, each driven at a frequency close to its first normal mode. Red filled circles and black filled squares indicate the boundary points of each region, and the connecting lines are drawn only to guide the eye. Note the logarithmic scale: the parameter space in which recurrence is observed becomes significantly narrower for $N = 32$ compared to $N = 8$.

B. Recurrence regions versus chain Length

Finally, we investigated how the recurrence regions depend on the chain length. Given many parameters in the model, we fixed the nonlinear coupling coefficient at $\alpha = 0.25$ and performed scans in the driving amplitude–damping plane separately for chains of length $N = 8, 16$, and 32, using a fixed driving frequency near mode 1, respectively. As shown in Fig. 7, the parameter space in which recurrence is observed becomes significantly narrower with increasing chain length. For $N = 32$, the maximum damping that allows such recurrence is about 5×10^{-5} , which already represents a very stringent requirement for realistic physical systems. This suggests that, in the thermodynamic limit ($N \rightarrow \infty$), such recurrence behavior is unlikely to persist.

IV. DISCUSSION AND CONDUCTION

We report numerical evidence of recurrence phenomena in α -FPUT chains. Similar investigations were carried out for β -FPUT chains, but no analogous recurrence was found within the finite parameter space we explored ($\beta = 8$). Moreover, since the driven FPUT problem is a prototypical multimode system with nonlinear mode coupling, deriving analytical approximations that describe the system's behavior inside the recurrence regions remains challenging, providing a natural direction for future theoretical exploration.

Interestingly, this long-time recurrence bears a superficial resemblance to phenomena recently studied in the context of discrete time crystals (DTCs)[26–28]. The periodic drive defines a discrete time-translation symmetry group generated by the operation $\mathcal{T}_T : t \mapsto t+T$. A discrete time crystal corresponds to a spontaneous breaking of this symmetry, where the system's response becomes periodic with an integer multiple of the driving period, i.e., a subgroup of the original time-translation group. In contrast, the long-period recurrence observed in our driven FPUT chain does not represent such symmetry breaking, because its recurrence period is not an integer multiple of the driving period, and the corresponding operation does not form a subgroup of the original symmetry group defined by the drive.

Nonetheless, this comparison highlights an intriguing analogy. The recurrence windows identified here can be regarded as a generalized, relaxed form of time-crystalline order, in which the system exhibits long-term temporal organization and approximate subharmonic responses. Understanding whether such structured recurrence can persist or be stabilized under modified conditions, such as weak noise, feedback control, or quasi-periodic driving, could provide a new bridge between classical nonlinear lattice dynamics and the emerging physics of time crystals, suggesting that classical multimode recurrence phenomena may serve as a testbed for exploring time-crystalline-like behavior.

Finally, returning to the original motivation of this work, our results indicate that FPUT recurrence phenomena, traditionally studied in isolated Hamiltonian systems, can also manifest in driven, open systems accessible in laboratory experiments.

ACKNOWLEDGMENTS

This research was supported by the Research Project Supported by Shanxi Scholarship Council of China (Grant No. 2023-033), and the Fundamental Research Program of Shanxi Province (Grant No. 202303021221071).

- [1] E. Fermi, P. Pasta, S. Ulam, and M. Tsingou, *STUDIES OF THE NONLINEAR PROBLEMS*, Tech. Rep. (Los Alamos Scientific Lab., N. Mex., 1955).
- [2] T. Dauxois, M. Peyrard, and S. Ruffo, The fermi–pasta–ulam ‘numerical experiment’: history and pedagogical perspectives, *European Journal of Physics* **26**, S3 (2005).
- [3] G. P. Berman and F. M. Izrailev, The fermi–pasta–ulam problem: Fifty years of progress, *Chaos: An Interdisciplinary Journal of Nonlinear Science* **15**, 015104 (2005).
- [4] M. A. Porter, N. J. Zabusky, B. Hu, and D. K. Campbell, Fermi, pasta, ulam and the birth of experimental mathematics, *American Scientist* **97**, 214 (2009).
- [5] A. Ponomorov, H. Christodoulidi, C. Skokos, and S. Flach, The two-stage dynamics in the fermi-pasta-ulam problem: From regular to diffusive behavior, *Chaos: An Interdisciplinary Journal of Nonlinear Science* **21**, 043127 (2011).
- [6] M. Onorato, L. Vozella, D. Proment, and Y. V. Lvov, Route to thermalization in the α -fermi-pasta-ulam system, *Proceedings of the National Academy of Sciences* **112**, 4208 (2015).
- [7] G. M. Lando and S. Flach, Prethermalization in fermi-pasta-ulam-tsingou chains, *Phys. Rev. E* **112**, 014206 (2025).
- [8] R. Hirota and K. Suzuki, Studies on lattice solitons by using electrical networks, *Journal of the Physical Society of Japan* **28**, 1366 (1970).
- [9] S. Trillo, G. Deng, G. Biondini, M. Klein, G. F. Clauss, A. Chabchoub, and M. Onorato, Experimental observation and theoretical description of multisoliton fission in shallow water, *Phys. Rev. Lett.* **117**, 144102 (2016).
- [10] M. Wu and C. E. Patton, Experimental observation of fermi-pasta-ulam recurrence in a nonlinear feedback ring system, *Phys. Rev. Lett.* **98**, 047202 (2007).
- [11] C. Bao, J. A. Jaramillo-Villegas, Y. Xuan, D. E. Leaird, M. Qi, and A. M. Weiner, Observation of fermi-pasta-ulam recurrence induced by breather solitons in an optical microresonator, *Phys.*

- Rev. Lett.* **117**, 163901 (2016).
- [12] G. Van Simaey, P. Emplit, and M. Haelterman, Experimental demonstration of the fermi-pasta-ulam recurrence in a modulationally unstable optical wave, *Phys. Rev. Lett.* **87**, 033902 (2001).
- [13] A. Mussot, C. Naveau, M. Conforti, A. Kudlinski, F. Copie, P. Szriftgiser, and S. Trillo, Fibre multi-wave mixing combs reveal the broken symmetry of Fermi-Pasta-Ulam recurrence, *Nature Photonics* **12**, 303 (2018).
- [14] D. Pierangeli, M. Flammini, L. Zhang, G. Marcucci, A. J. Agranat, P. G. Grinevich, P. M. Santini, C. Conti, and E. DelRe, Observation of fermi-pasta-ulam-tingou recurrence and its exact dynamics, *Phys. Rev. X* **8**, 041017 (2018).
- [15] A. Mussot, A. Kudlinski, M. Droques, P. Szriftgiser, and N. Akhmediev, Fermi-pasta-ulam recurrence in nonlinear fiber optics: The role of reversible and irreversible losses, *Phys. Rev. X* **4**, 011054 (2014).
- [16] K. Geist and W. Lauterborn, The nonlinear dynamics of the damped and driven toda chain: I. energy bifurcation diagrams, *Physica D: Nonlinear Phenomena* **31**, 103 (1988).
- [17] Z. G. Nicolaou and A. E. Motter, Anharmonic classical time crystals: A coresonance pattern formation mechanism, *Phys. Rev. Res.* **3**, 023106 (2021).
- [18] D. Cai, A. Sánchez, A. R. Bishop, F. Falo, and L. M. Floría, Possible soliton motion in ac-driven damped nonlinear lattices, *Phys. Rev. B* **50**, 9652 (1994).
- [19] R. Khomeriki, S. Lepri, and S. Ruffo, Pattern formation and localization in the forced-damped fermi-pasta-ulam lattice, *Phys. Rev. E* **64**, 056606 (2001).
- [20] D. Cubero, J. Cuevas, and P. G. Kevrekidis, Nucleation of breathers via stochastic resonance in nonlinear lattices, *Phys. Rev. Lett.* **102**, 205505 (2009).
- [21] J. Cuevas, L. Q. English, P. G. Kevrekidis, and M. Anderson, Discrete breathers in a forced-damped array of coupled pendula: Modeling, computation, and experiment, *Phys. Rev. Lett.* **102**, 224101 (2009).
- [22] G. Bel, B. S. Alexandrov, A. R. Bishop, and K. O. Rasmussen, Double-period breathers in a driven and damped lattice, *Phys. Rev. E* **98**, 062205 (2018).
- [23] A. Nayfeh and D. Mook, *Nonlinear Oscillations* (Wiley, 2024).
- [24] S. Ciliberto and J. P. Gollub, Pattern competition leads to chaos, *Phys. Rev. Lett.* **52**, 922 (1984).

- [25] L. Bello, M. Calvanese Strinati, E. G. Dalla Torre, and A. Pe'er, Persistent coherent beating in coupled parametric oscillators, [Phys. Rev. Lett. **123**, 083901 \(2019\)](#).
- [26] N. Y. Yao and C. Nayak, Time crystals in periodically driven systems, [Physics Today **71**, 40 \(2018\)](#).
- [27] T. L. Heugel, M. Oscity, A. Eichler, O. Zilberberg, and R. Chitra, Classical many-body time crystals, [Phys. Rev. Lett. **123**, 124301 \(2019\)](#).
- [28] N. Y. Yao, C. Nayak, L. Balents, and M. P. Zaletel, Classical discrete time crystals, [Nature Physics **16**, 438 \(2020\)](#).